Cyanoacetylene in the outflow/hot molecular core G331.512-0.103

Duronea N.U.
Bronfman L.
Mendoza E.
Merello M.
Finger R.
Reyes N.
Hervias-Caimapo C.
Faure A.
Cappa C.
Arnal E.M.
Lépine J.R.D.
Kleiner I.
Nyman L-A.

ALLAM 2019. Astrochemistry LLAMA Meeting. Sao Paulo, August 8-9 2019. IAG-USP

Schematic of a Hot Core

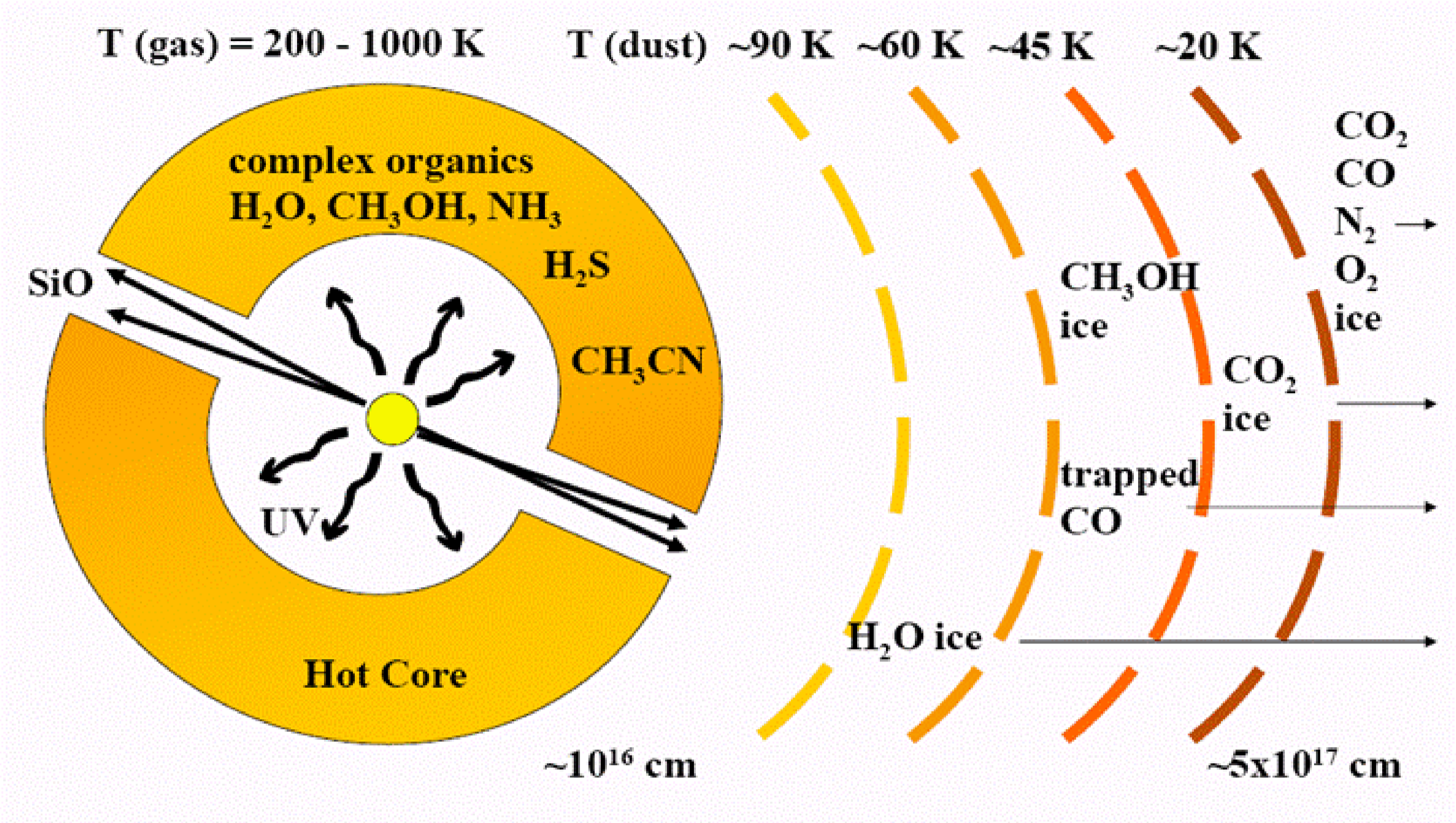

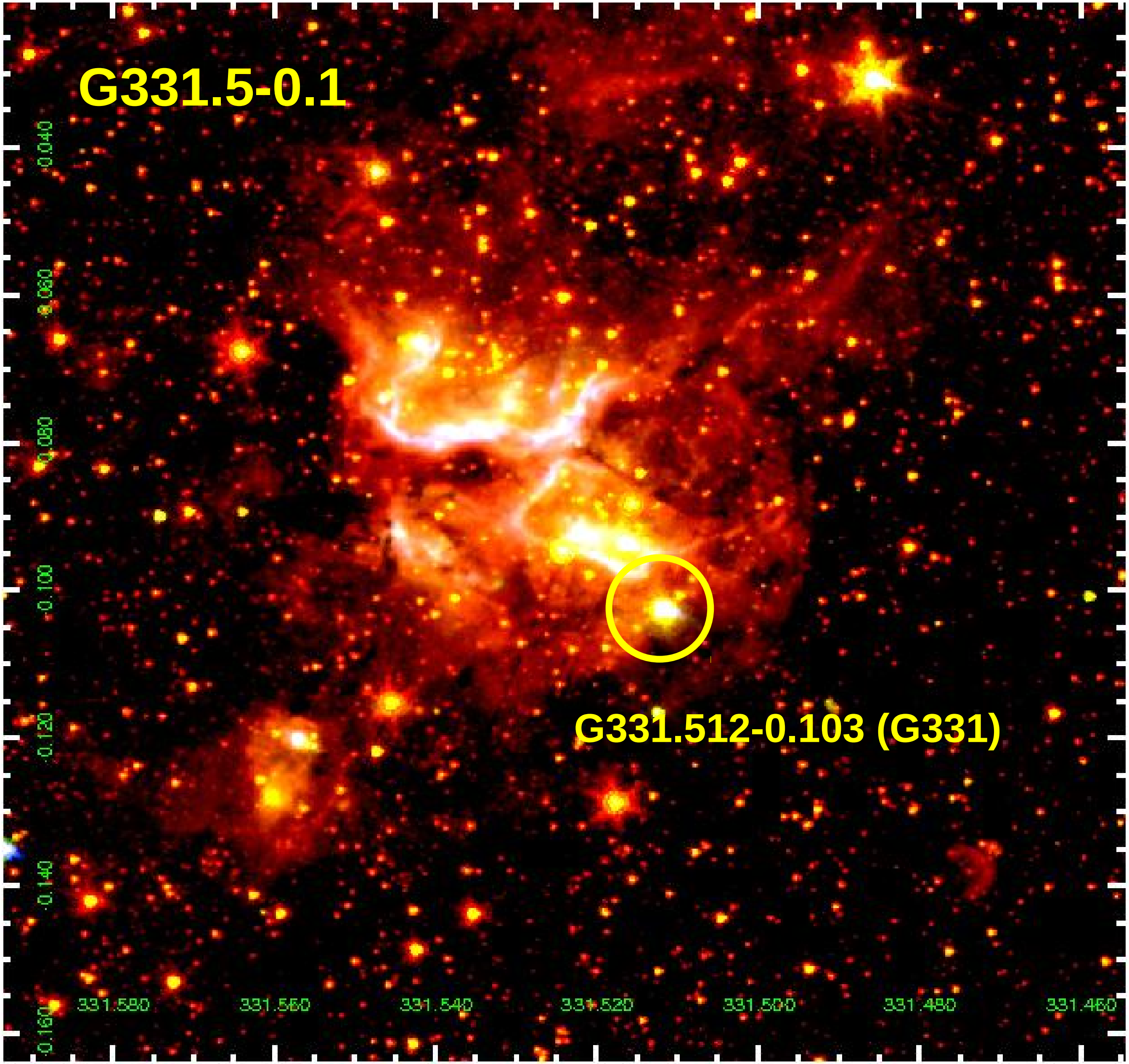
G331.5-0.1
G331.512-0.103 (G331)
-0.040
-0.060
-0.080
-0.100
-0.120
-0.140
-0.160
331.580
331.560
331.540
331.520
331.500
331.480
331.460


The Astrophysical Journal, 672:391–397, 2008 January 1

DISCOVERY OF AN EXTREMELY HIGH VELOCITY, MASSIVE, AND COMPACT MOLECULAR OUTFLOW IN NORMA

Leonardo Bronfman, Guido Garay, Manuel Merello, Diego Mardones, and Jorge May

Kate J. Brooks

Lars-Åke Nyman

and

Rolf Güsten


The Astrophysical Journal, 774:38 (20pp), 2013 September 1

PHYSICAL CHARACTERISTICS OF G331.5-0.1: THE LUMINOUS CENTRAL REGION OF A GIANT MOLECULAR CLOUD

Manuel Merello, Leonardo Bronfman, Guido Garay, Lars-Åke Nyman, Neal J. Evans II, and C. Malcolm Walmsley


The Astrophysical Journal Letters, 774:L7 (6pp), 2013 September 1

ALMA OBSERVATIONS OF THE MASSIVE MOLECULAR OUTFLOW G331.512−0.103

Manuel Merello, Leonardo Bronfman, Guido Garay, Nadia Lo, Neal J. Evans II, Lars-Åke Nyman, Juan R. Cortés, and Maria R. Cunningham


Draft version December 27, 2018

arXiv:1812.09779v1 [astro-ph.GA] 23 Dec 2018

ALMA OBSERVATIONS OF THE MASSIVE MOLECULAR OUTFLOW G331.512-0.103 II: PHYSICAL PROPERTIES, KINEMATICS, AND GEOMETRY MODELING

Carlos Hervías-Caimapo, Manuel Merello, Leonardo Bronfman, Lars-Åke Nyman, Guido Garay, Nadia Lo, Neal J. Evans II, Cristian López-Calderón, and Edgar Mendoza


The Astrophysical Journal, 853:152 (12pp), 2018 February 1

G331.512–0.103: An Interstellar Laboratory for Molecular Synthesis. I. The Ortho-to-para Ratios for CH_3OH and CH_3CN

Edgar Mendoza, Leonardo Bronfman, Nicolas U. Duronea, Jacques R. D. Lépine, Ricardo Finger, Manuel Merello, Carlos Hervías-Caimapo, Diana R. G. Gama, Nicolas Reyes, and Lars Åke-Nyman

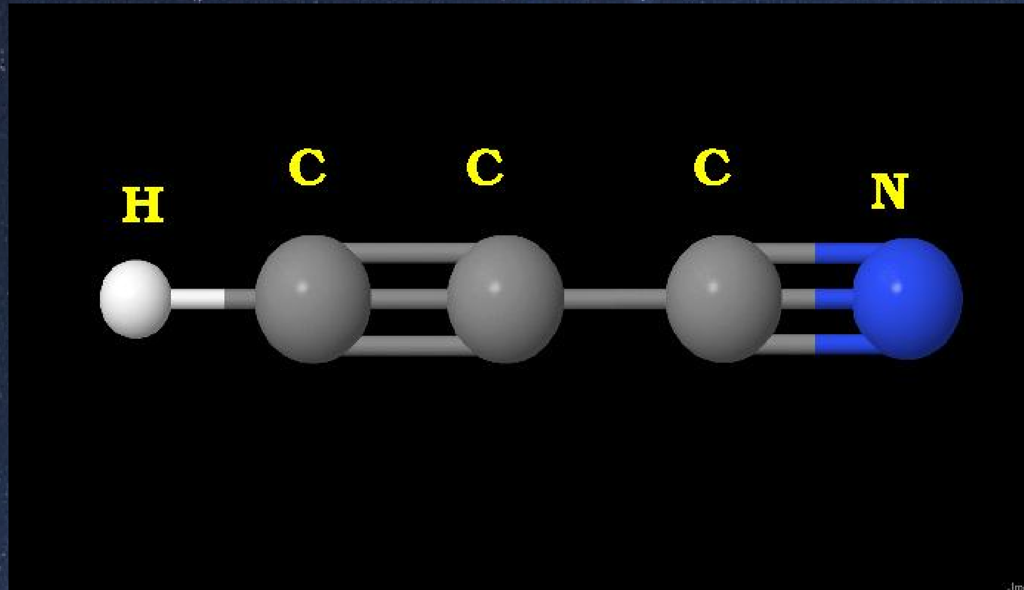

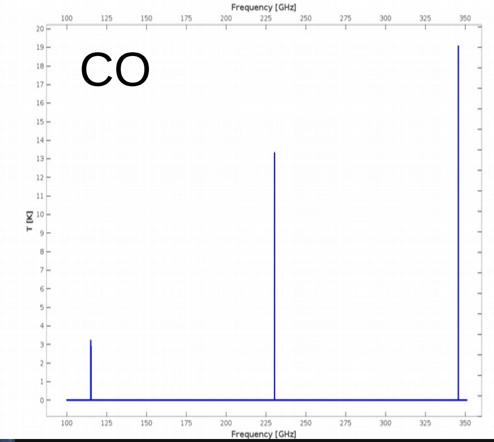

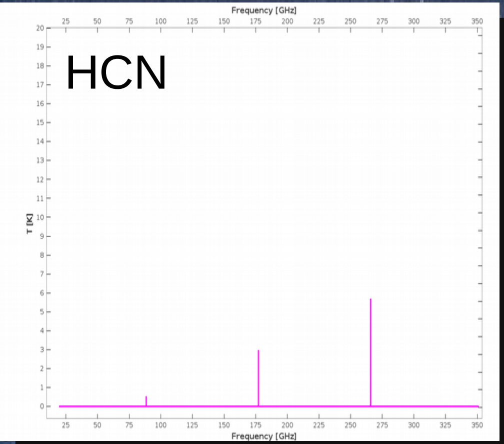

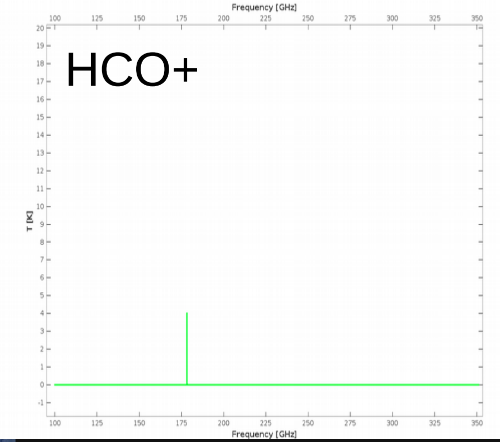

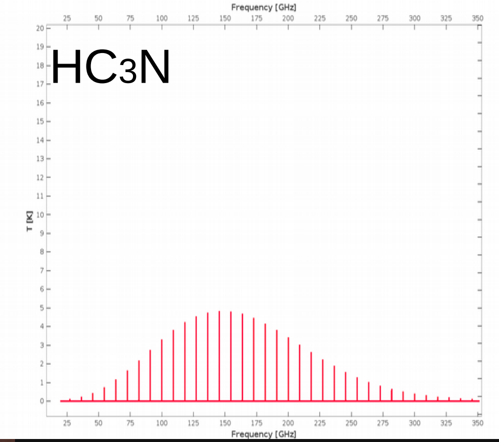

ALLAM 2019. Astrochemistry LLAMA Meeting. Sao Paulo, August 8-9 2019. IAG-USP

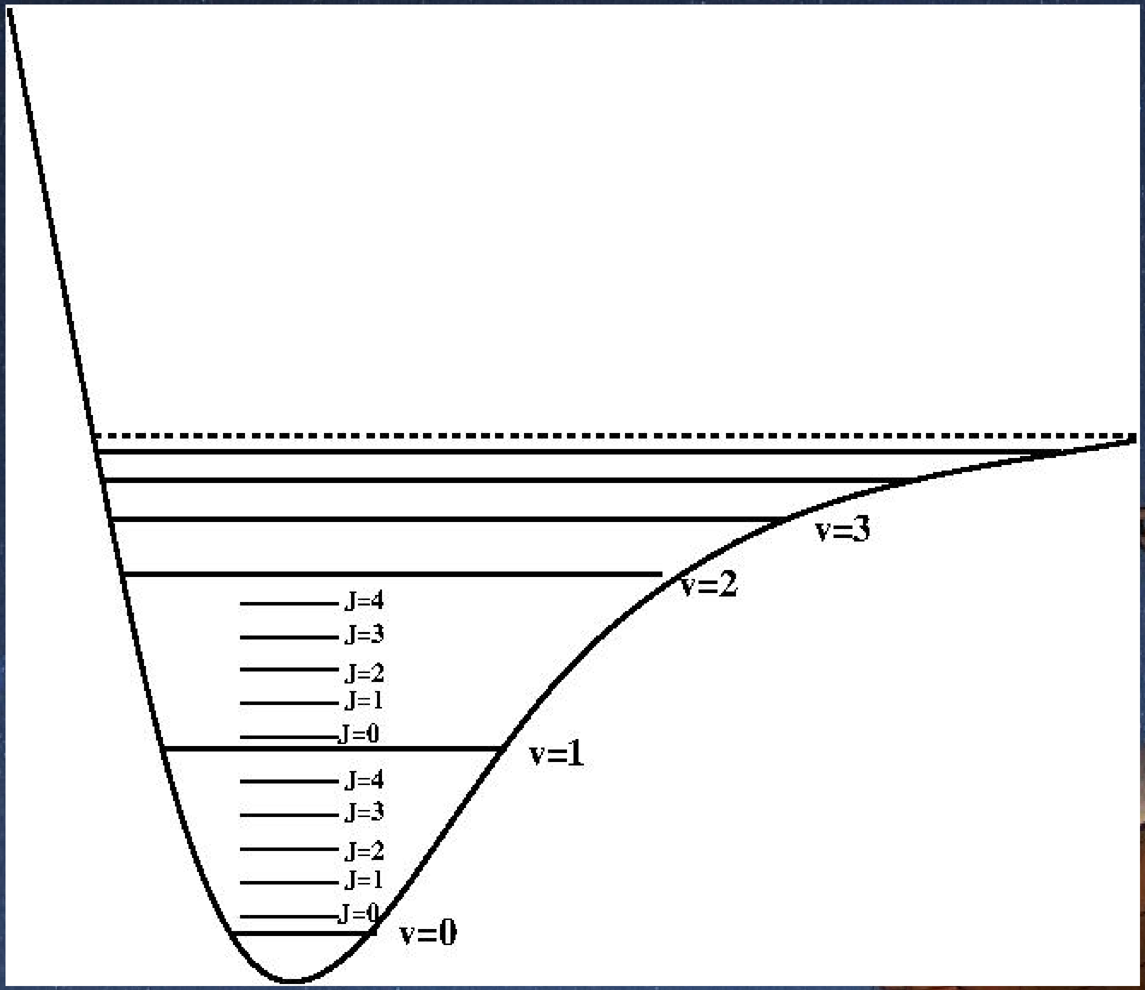
v=3
v=2
J=4
J=3
J=2
J=1
J=0
v=1
J=4
J=3
J=2
J=1
J=0
v=0

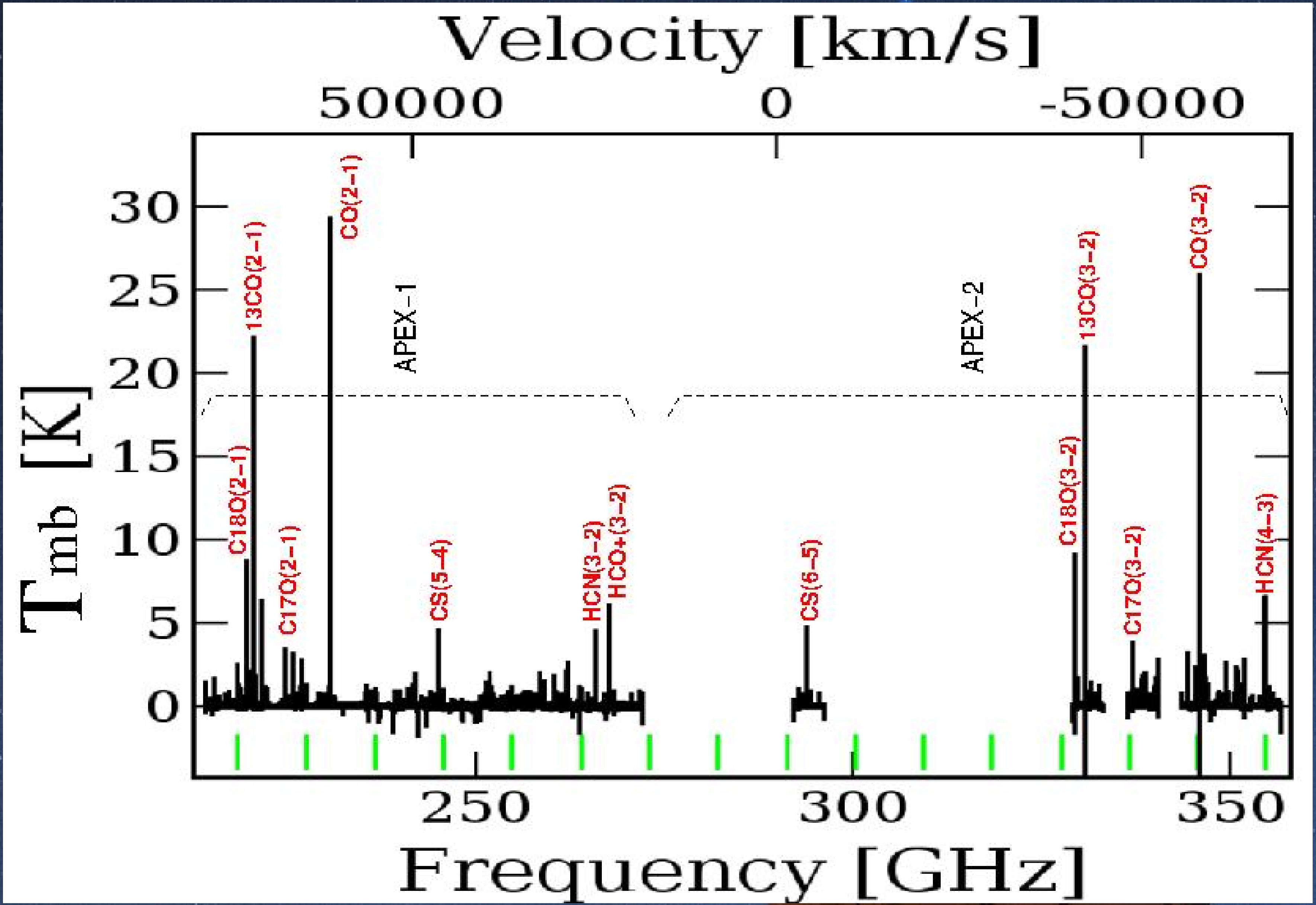
Velocity [km/s]
50000
0
-50000
30
25
20
15
10
5
0
Tmb [K]
13CO(2–1)
CO(2–1)
APEX–1
APEX–2
13CO(3–2)
CO(3–2)
C18O(2–1)
C17O(2–1)
CS(5–4)
HCN(3–2)
HCO+(3–2)
CS(6–5)
C18O(3–2)
C17O(3–2)
HCN(4–3)
250
300
350
Frequency [GHz]

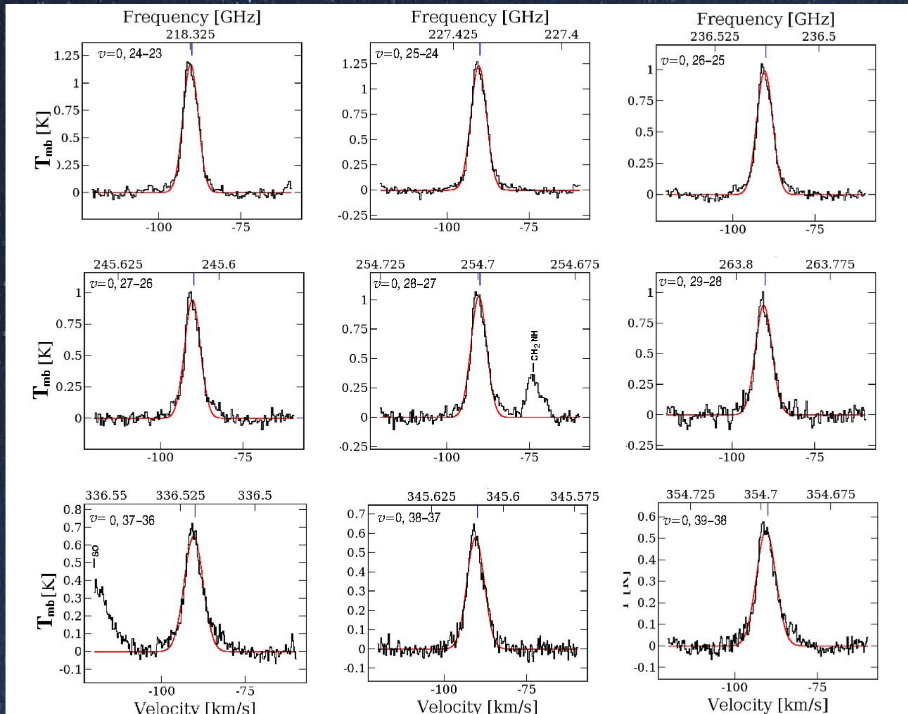
Frequency [GHz]
v=0, 24–23
v=0, 25–24
v=0, 26–25
v=0, 27–26
v=0, 28–27
CH_2NH
v=0, 29–28
v= 0, 37–36
SO
v=0, 38–37
v=0, 39–38
T_{mb} [K]
Velocity [km/s]

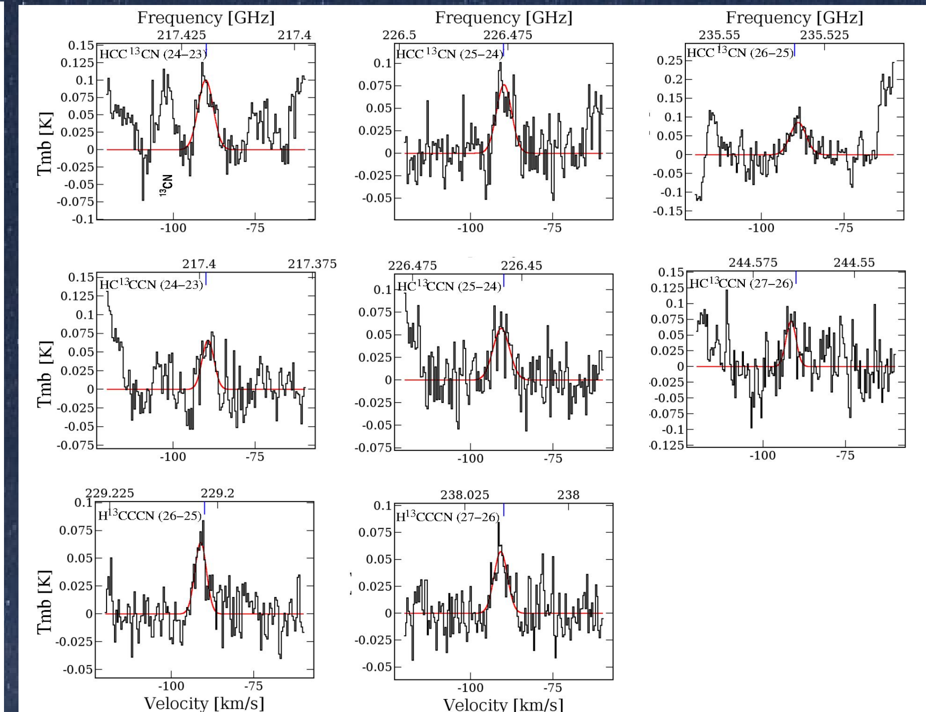
Frequency [GHz]
$HCC^{13}CN$ (24–23)
^{13}CN
$HCC^{13}CN$ (25–24)
$HCC^{13}CN$ (26–25)
$HC^{13}CCN$ (24–23)
$HC^{13}CCN$ (25–24)
$HC^{13}CCN$ (27–26)
$H^{13}CCCN$ (26–25)
$H^{13}CCCN$ (27–26)
Tmb [K]
Velocity [km/s]

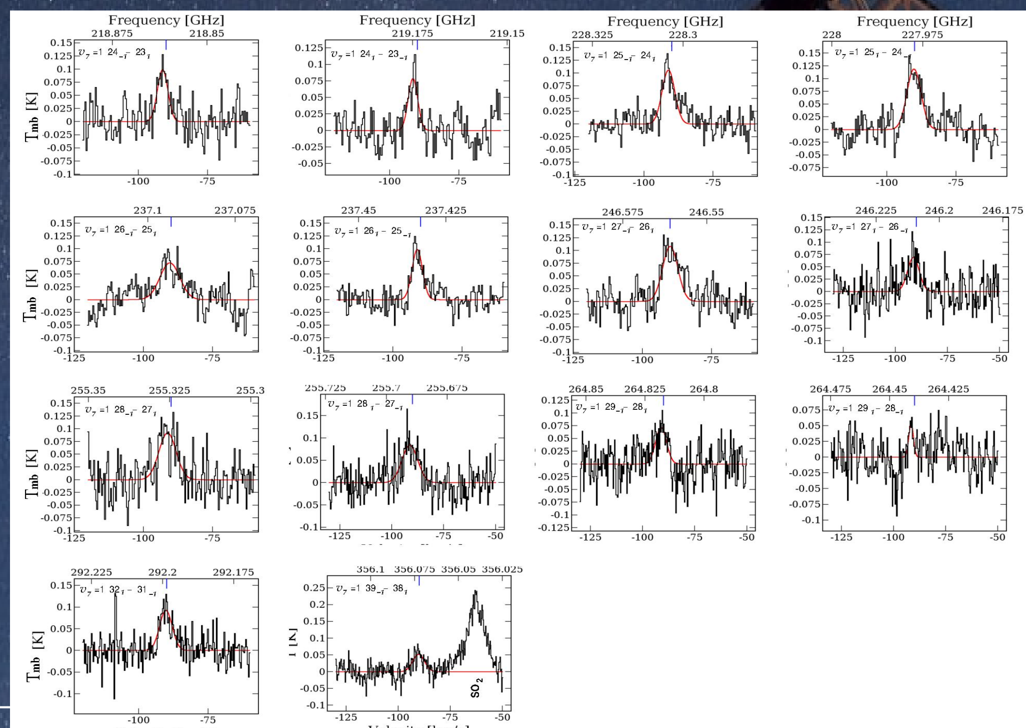
Frequency [GHz]
v_7=1 24_{-1} – 23_1
v_7=1 24_1 – 23_{-1}
v_7=1 25_{-1} – 24_1
v_7=1 25_1 – 24_{-1}
v_7=1 26_{-1} – 25_1
v_7=1 26_1 – 25_{-1}
v_7=1 27_{-1} – 26_1
v_7=1 27_1 – 26_{-1}
v_7=1 28_{-1} – 27_1
v_7=1 28_1 – 27_{-1}
v_7=1 29_{-1} – 28_1
v_7=1 29_1 – 28_{-1}
v_7=1 32_1 – 31_{-1}
v_7=1 39_{-1} – 38_1
SO_2
T_{mb} [K]
Velocity [km/s]

Table 1. HC_3N lines detected in G331 and their parameters obtained from Gaussian fits.

Transition	Frequency (MHz)	E_u (K)	A_{ul} ($\times 10^{-5} s^{-1}$)	$\int T_{mb}\,dv$ (K km s^{-1})	V_{lsr} (km s^{-1})	T_{peak} (K)	FWHM (km s^{-1})	τ	Remark§
$v = 0$									
24–23	218324.72	130.98	82.6	6.94 ± 0.72	-90.35 ± 0.05	1.17 ± 0.05	5.39 ± 0.11	0.298*	cl
25–24	227418.91	141.89	93.5	7.49 ± 0.75	-90.37 ± 0.05	1.23 ± 0.05	5.57 ± 0.11	0.278*	cl
26–25	236512.78	153.24	105.2	6.20 ± 0.62	-90.35 ± 0.05	0.99 ± 0.04	5.55 ± 0.12	0.260*	cl
27–26	245606.31	165.03	117.9	6.02 ± 0.61	-90.37 ± 0.07	0.94 ± 0.06	5.63 ± 0.17	0.248*	cl
28–27	254699.51	177.25	131.6	6.47 ± 0.66	-90.37 ± 0.07	1.02 ± 0.06	5.58 ± 0.15	0.235*	pbw $^{33}SO_2$ nl CH_2NH
29–28	263792.31	189.91	146.3	5.85 ± 0.59	-90.49 ± 0.07	0.89 ± 0.06	5.93 ± 0.16	0.206*	pbw CH_3OH
37–36	336520.08	306.91	304.8	4.86 ± 0.50	-90.50 ± 0.08	0.65 ± 0.05	6.67 ± 0.19	0.082*	nl SO
38–37	345609.01	323.49	330.2	3.87 ± 0.39	-90.57 ± 0.06	0.58 ± 0.04	6.16 ± 0.14	0.077*	pbw CH_3OH
39–38	354697.46	340.51	357.1	4.14 ± 0.43	-90.54 ± 0.08	0.53 ± 0.04	6.92 ± 0.18	0.060*	cl
^{13}C Isotopologues									
$H^{13}CCCN$									
26–25	229203.09	148.51	95.7	0.28 ± 0.04	-91.1 ± 0.2	0.06 ± 0.02	4.1 ± 0.4	0.024†	cl
27–26	238015.68	159.93	197.3	0.30 ± 0.04	-90.9 ± 0.2	0.06 ± 0.02	4.8 ± 0.5	0.022†	cl
$HC^{13}CCN$									
24–23	217398.56	130.42	81.5	0.28 ± 0.05	-89.4 ± 0.4	0.07 ± 0.02	4.2 ± 0.8	0.025†	cl
25–24	226454.18	141.29	92.3	0.32 ± 0.05	-90.7 ± 0.4	0.06 ± 0.02	5.9 ± 1.0	0.024†	cl
27–26	244564.44	164.33	116.4	0.32 ± 0.06	-91.5 ± 0.4	0.07 ± 0.03	3.6 ± 0.8	0.027†	pbw CH_3OH
$HCC^{13}CN$									
24–23	217419.57	130.44	81.6	0.51 ± 0.06	-90.2 ± 0.2	0.10 ± 0.02	5.4 ± 0.4	0.035†	pbw CH_3OH nl ^{13}CN
25–24	226476.04	141.31	92.3	0.43 ± 0.06	-89.9 ± 0.4	0.08 ± 0.03	5.4 ± 0.7	0.031†	cl
26–25	235532.20	152.61	103.9	0.50 ± 0.07	-88.9 ± 0.3	0.09 ± 0.02	5.6 ± 0.6	0.037†	cl
$v_7 = 1$									
$24_{-1}–23_{1}$	218860.81	452.15	82.7	0.58 ± 0.07	-91.3 ± 0.3	0.10 ± 0.03	4.9 ± 0.5	0.015*	cl
$24_{1}–23_{-1}$	219173.75	452.34	83.0	0.34 ± 0.05	-91.6 ± 0.3	0.08 ± 0.02	4.1 ± 0.6	0.018*	cl
$25_{1}–24_{-1}$	227977.27	463.09	93.5	0.69 ± 0.08	-90.2 ± 0.2	0.12 ± 0.02	6.0 ± 0.5	0.013*	cl
$25_{-1}–24_{1}$	228303.17	463.29	93.4	0.70 ± 0.09	-90.8 ± 0.3	0.10 ± 0.02	6.8 ± 0.6	0.011*	cl
$26_{-1}–25_{1}$	237093.38	474.47	105.2	0.53 ± 0.07	-90.5 ± 0.4	0.07 ± 0.02	8.4 ± 1.2	0.009*	cl
$26_{1}–25_{-1}$	237432.26	474.69	105.7	0.57 ± 0.07	-91.0 ± 0.2	0.10 ± 0.03	5.3 ± 0.5	0.014*	cl
$27_{1}–26_{-1}$	246209.14	486.29	118.0	0.45 ± 0.08	-91.4 ± 0.5	0.07 ± 0.03	9.0 ± 1.9	0.011*	cl
$27_{-1}–26_{1}$	246560.95	486.52	118.5	0.78 ± 0.10	-89.3 ± 0.4	0.10 ± 0.03	8.1 ± 0.9	0.009*	cl
$28_{-1}–27_{1}$	255324.55	498.54	131.7	0.58 ± 0.10	-91.5 ± 0.5	0.09 ± 0.03	6.7 ± 1.1	0.011*	cl
$28_{1}–27_{-1}$	255689.29	498.79	132.2	0.72 ± 0.11	-91.3 ± 0.6	0.08 ± 0.02	8.9 ± 1.6	0.008*	cl
$29_{1}–28_{-1}$	264439.58	511.23	146.4	0.20 ± 0.04	-91.6 ± 0.3	0.05 ± 0.03	2.6 ± 0.7	0.029*	cl
$29_{-1}–28_{1}$	264817.24	511.50	147.1	0.40 ± 0.07	-91.1 ± 0.5	0.07 ± 0.02	6.2 ± 1.1	0.012*	cl
$32_{1}–31_{-1}$	292198.64	552.26	197.9	0.50 ± 0.08	-90.2 ± 0.3	0.09 ± 0.02	4.9 ± 0.6	0.014*	cl
$39_{-1}–38_{1}$	356072.44	662.68	359.2	0.31 ± 0.06	-90.3 ± 0.4	0.05 ± 0.02	6.6 ± 1.0	0.008*	nlo SO_2

*Obtained iteratively from the opacity correction (Sect 4.2.1) †Obtained from Eq.8 (Sect. 4.2.3)

LTE analysis

$$N_u = \frac{8\pi k \nu^2}{h c^3 A_{ul}} \times \int T_{\rm mb}\ dv$$

$$\ln\left(\frac{N_u}{g_u}\right) = \ln\left(\frac{N_{\rm tot}}{Q(T_{\rm exc})}\right) - \frac{E_u}{kT_{\rm exc}}$$

y = B + Ax

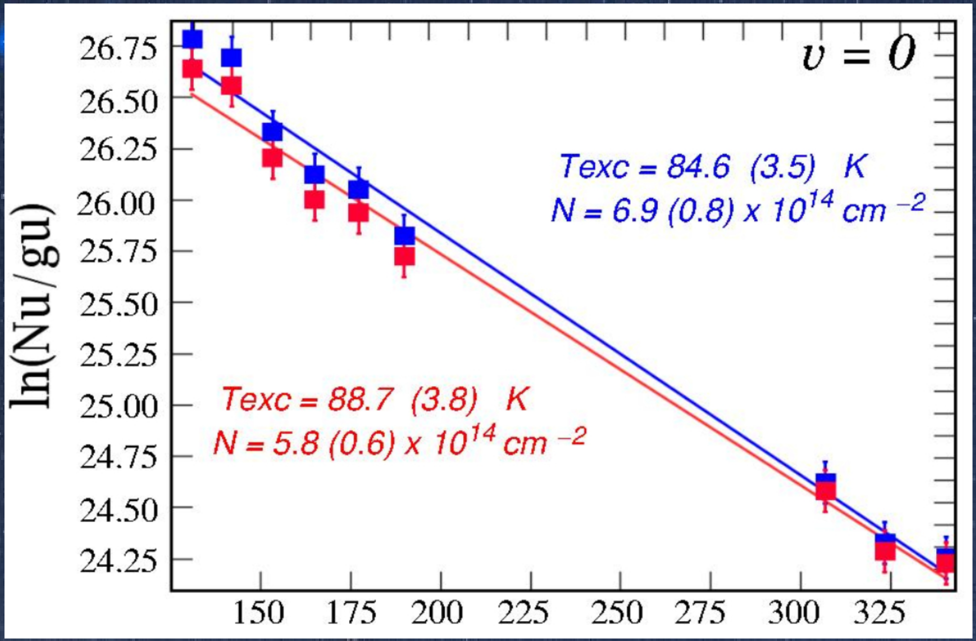

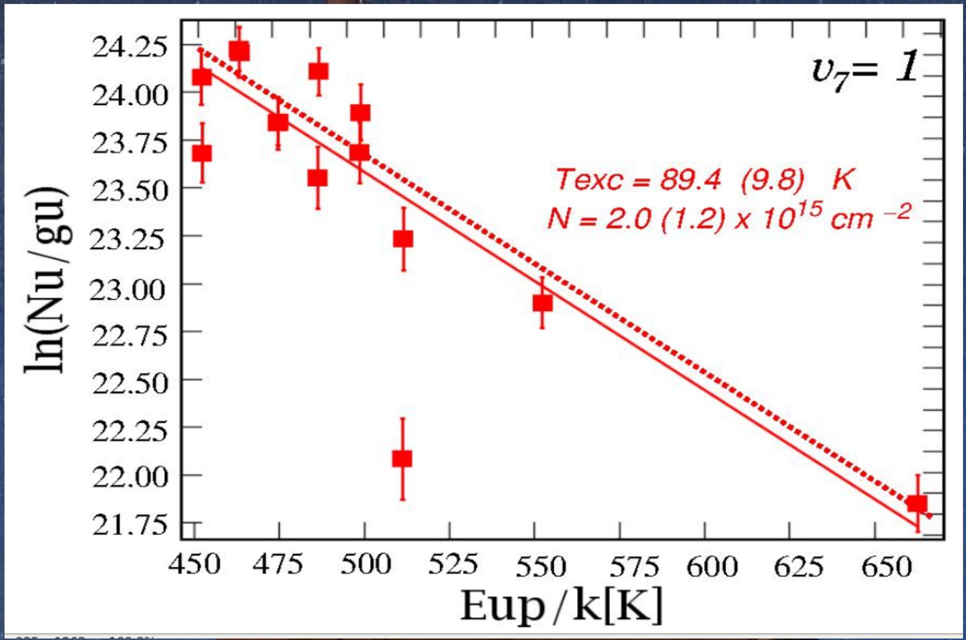

Non-LTE analysis

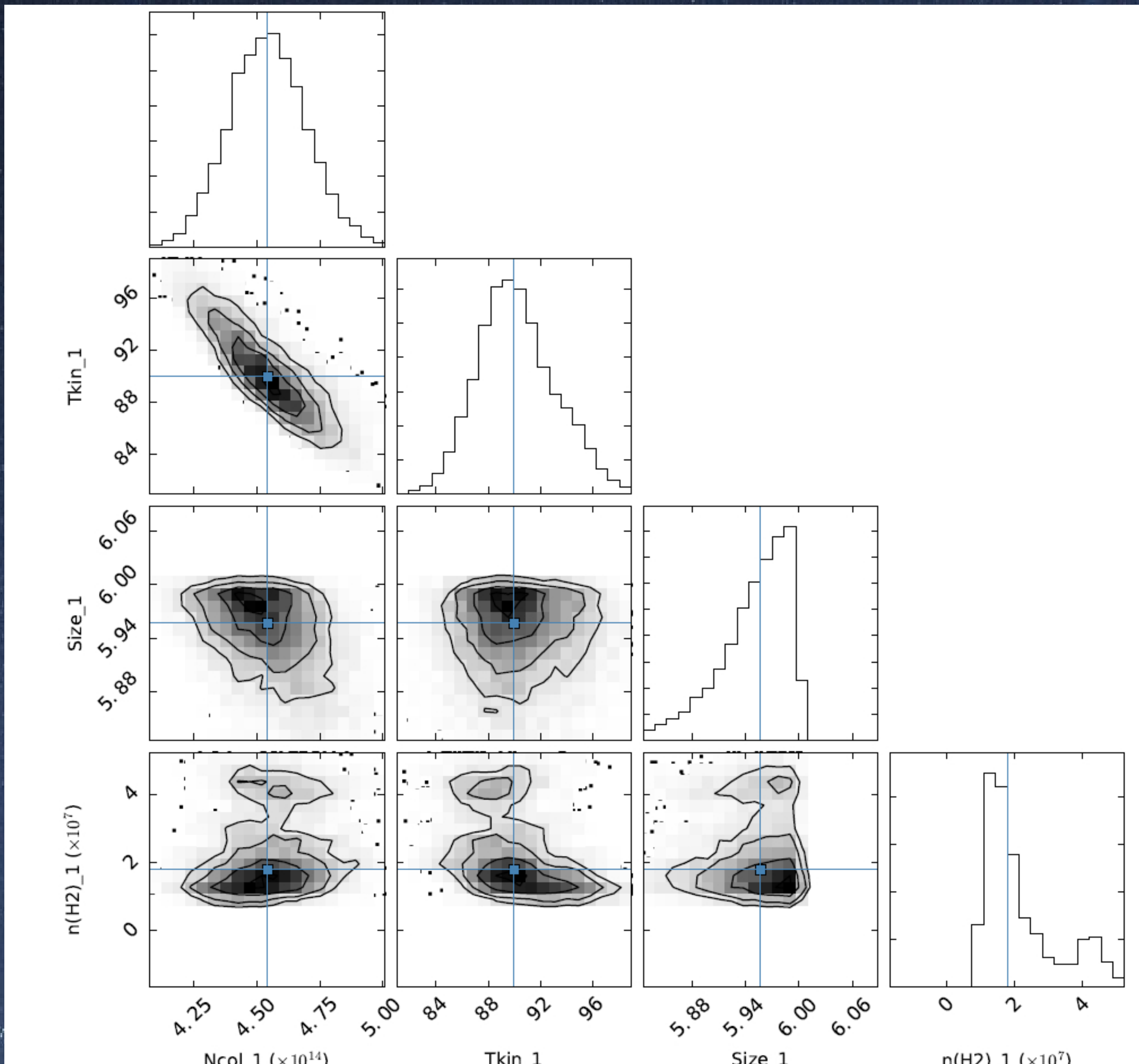

$N(HC_3N) = 4.5 \times 10^{14}\ cm^{-2}$

Tkin= 90 K

$n(H_2) = 2 \times 10^{7}\ cm^{-3}$

(size <= 6")

^{13}C Isotopologues

$$\tau = -\ln\left[1 - \frac{T_{\rm mb}}{f\,[J(T_{\rm exc}) - J(T_{\rm bg})]}\right] \quad (8)$$

being

$$J(T) = \frac{h\nu}{k}\left[e^{\left(\frac{h\nu}{kT}\right)} - 1\right]^{-1}, \quad (9)$$

and

$$N = \tau\,\frac{3h\Delta v}{8\pi^3}\sqrt{\frac{\pi}{4\ \ln 2}}\,\frac{Q}{\mu^2(J_l+1)}\ e^{\left(\frac{E_l}{kT_{\rm exc}}\right)}\left[1 - e^{\left(-\frac{h\nu}{kT_{\rm exc}}\right)}\right]^{-1} \quad (10)$$

Isotopologue	N [$\times\ 10^{13}$ cm^{-2}]	X [$\times\ 10^{-11}$]	^{12}C/^{13}C
HC_3N	$69 \pm 8^{\dagger}$	$79 - 62$	-
$HCC^{13}CN$	6.7 ± 0.9	$7.8 - 5.9$	~ 10
$HC^{13}CCN$	3.8 ± 0.8	$4.7 - 3.1$	~ 18
$H^{13}CCCN$	3.7 ± 0.6	$4.4 - 3.2$	~ 19
$^{13}C\ HC_3N$	$3.3 \pm 0.2^{\ddagger}$	$3.6 - 3.2$	~ 21

Excitation of the v=0 and v_7=1 lines

$$n_c^{J,J-1} \approx \frac{A_{(J,J-1)}}{\gamma(J, J-1)}$$

J=38-37 n_c (80-100 K) ~ 1.5 x 10^7 cm^{-3}

n(RADEX)~2 x 10^7 cm^{-3}

→ rotational transitions in LTE

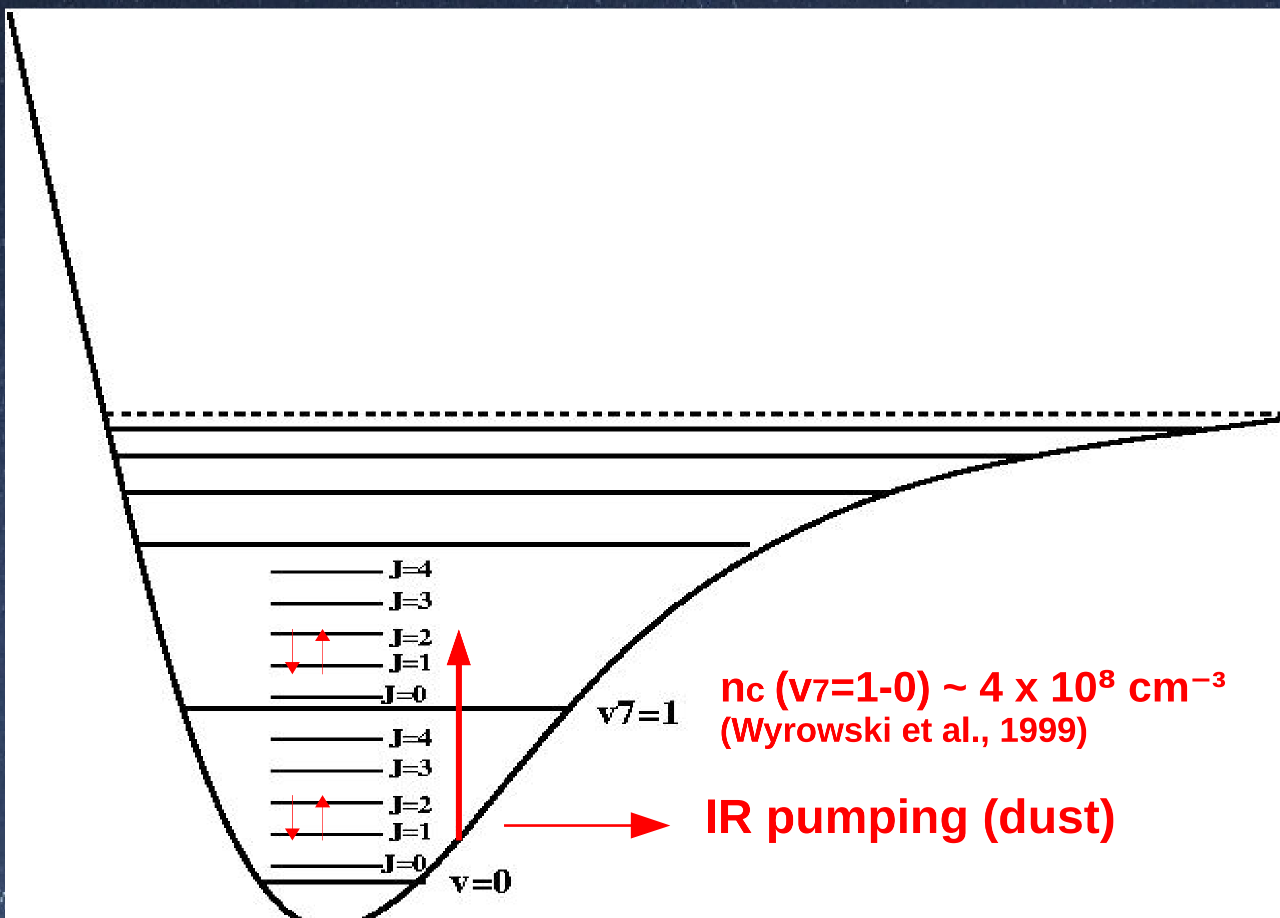

Excitation of the v=0 and v_7=1 lines

T_{dust} ~ T_{vib}

$$\frac{W_{(v_7=1)}}{W_{(v=0)}} = \exp\left(\frac{-\Delta E_{70}}{kT_{\rm vib}}\right)$$

T_{vib} = 140 K

$$\frac{L_{\rm hc}}{L_\odot} = 1.8625 \times 10^{-5}\left(\frac{r}{10^{16}\ {\rm cm}}\right)^2 T_{\rm dust}^4$$

L ~ 4 x 10^6 Lo

→ ***< O4 (ZAMS)***

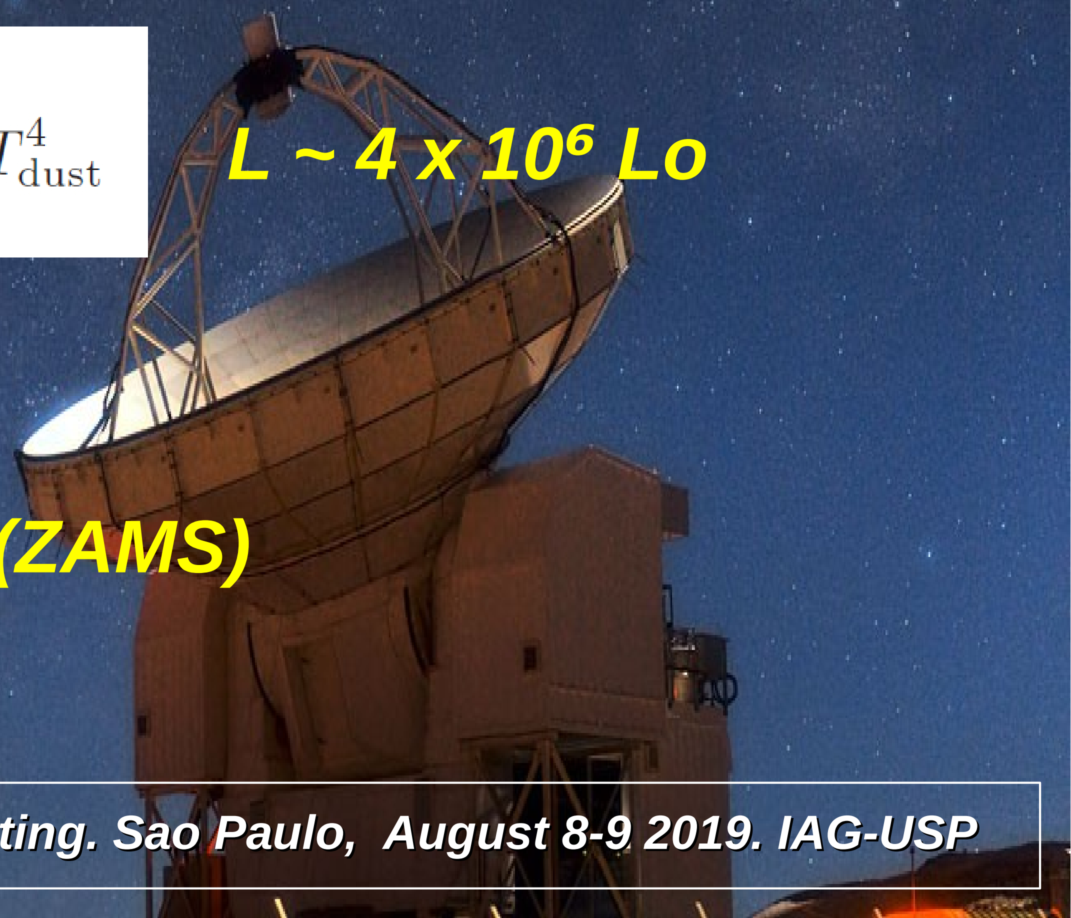

Isotopologue abundances

Isotopologue	N [$\times 10^{13}$ cm^{-2}]	X [$\times 10^{-11}$]	^{12}C/^{13}C
HC_3N	$69 \pm 8^{\dagger}$	79 – 62	-
$HCC^{13}CN$	6.7 ± 0.9	7.8 – 5.9	~ 10
$HC^{13}CCN$	3.8 ± 0.8	4.7 – 3.1	~ 18
$H^{13}CCCN$	3.7 ± 0.6	4.4 – 3.2	~ 19
$^{13}C\ HC_3N$	$3.3 \pm 0.2^{\ddagger}$	3.6 – 3.2	~ 21

$$[HCC^{13}CN]:[HC^{13}CCN]:[H^{13}CCCN] = 1.8(\pm 0.5):1.0:1.0(\pm 0.4)$$

$$C_2H_2 + CN \rightarrow HCCCN + H$$

$$H_2C_2 + {}^{13}CN \rightarrow HCC^{13}CN + H$$

$$[HCC^{13}CN]:[HC^{13}CCN]:[H^{13}CCCN] = a:b:c, \text{ with } a>b\approx c$$

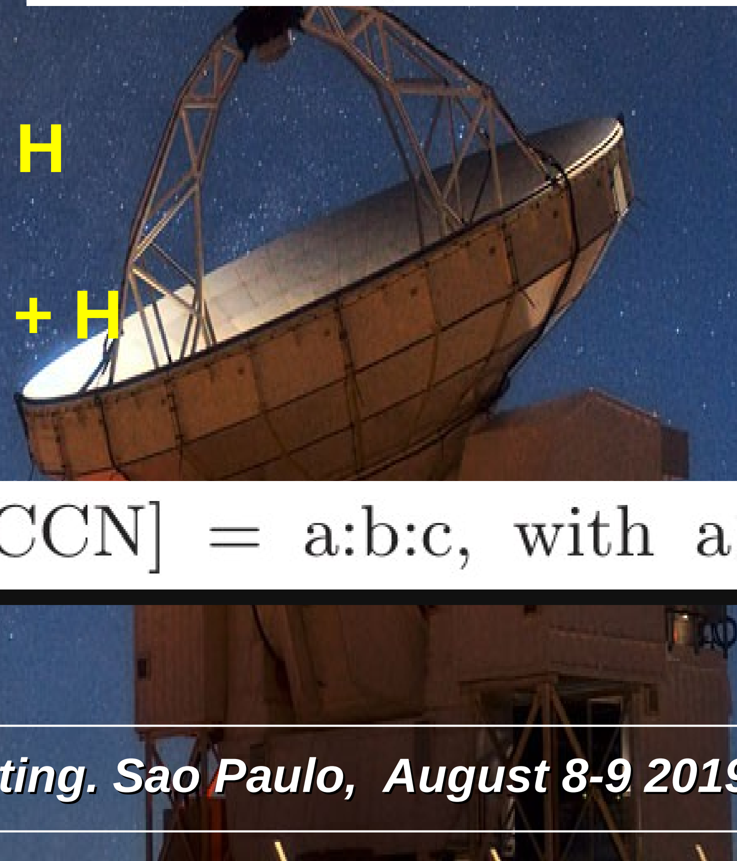

Isotopologue abundances

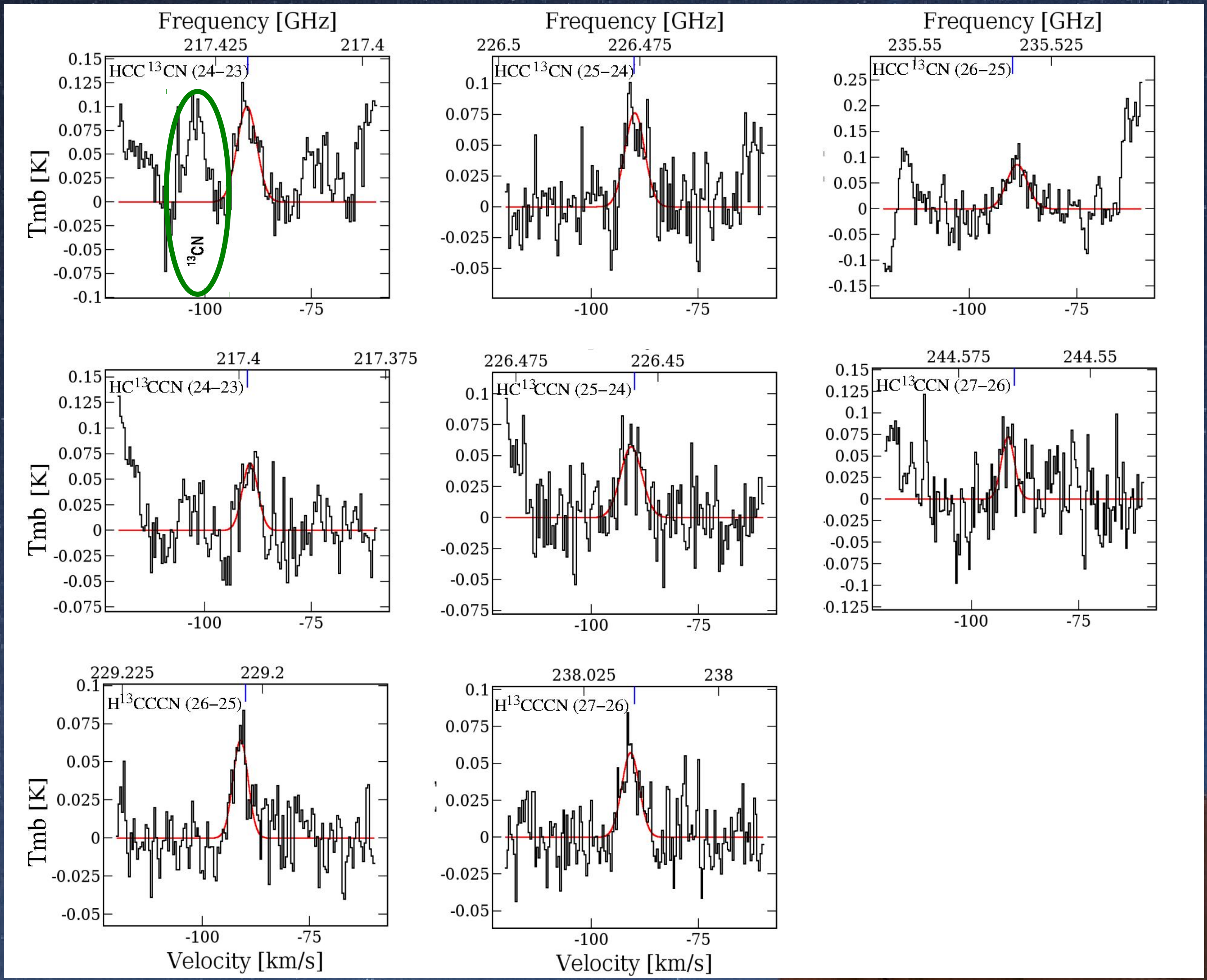

ALLAM 2019. Astrochemistry LLAMA Meeting. Sao Paulo, August 8-9 2019. IAG-USP

Emission of HC_3N

Merello et al. 2013

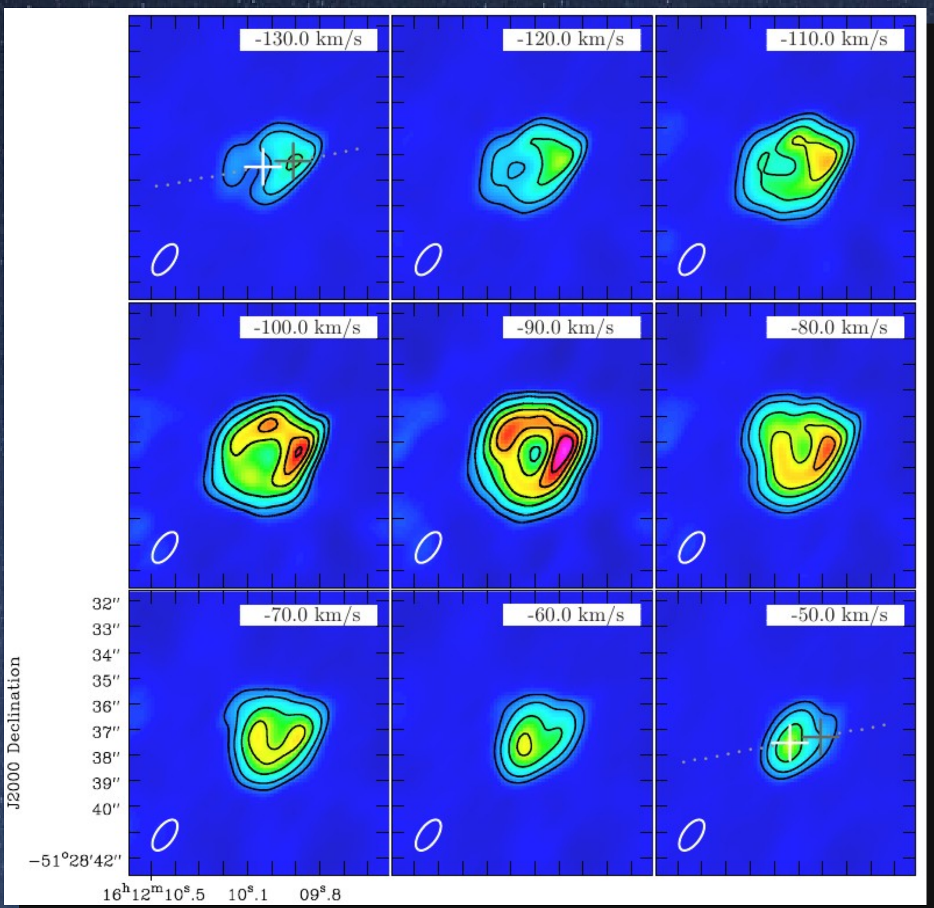

Hervias-Caimapo et al. 2019

SiO
$S^{18}O$
HCO+
$H^{13}CN$
HC_3N

“Broad” lines (~ 160-200 K)
(Shocked gas and outflow)

CH_3OH
CH_3CCH
$H^{13}CO$

“Narrow” lines (~ 70 K)
(colder ambient core)

Emission of HC_3N

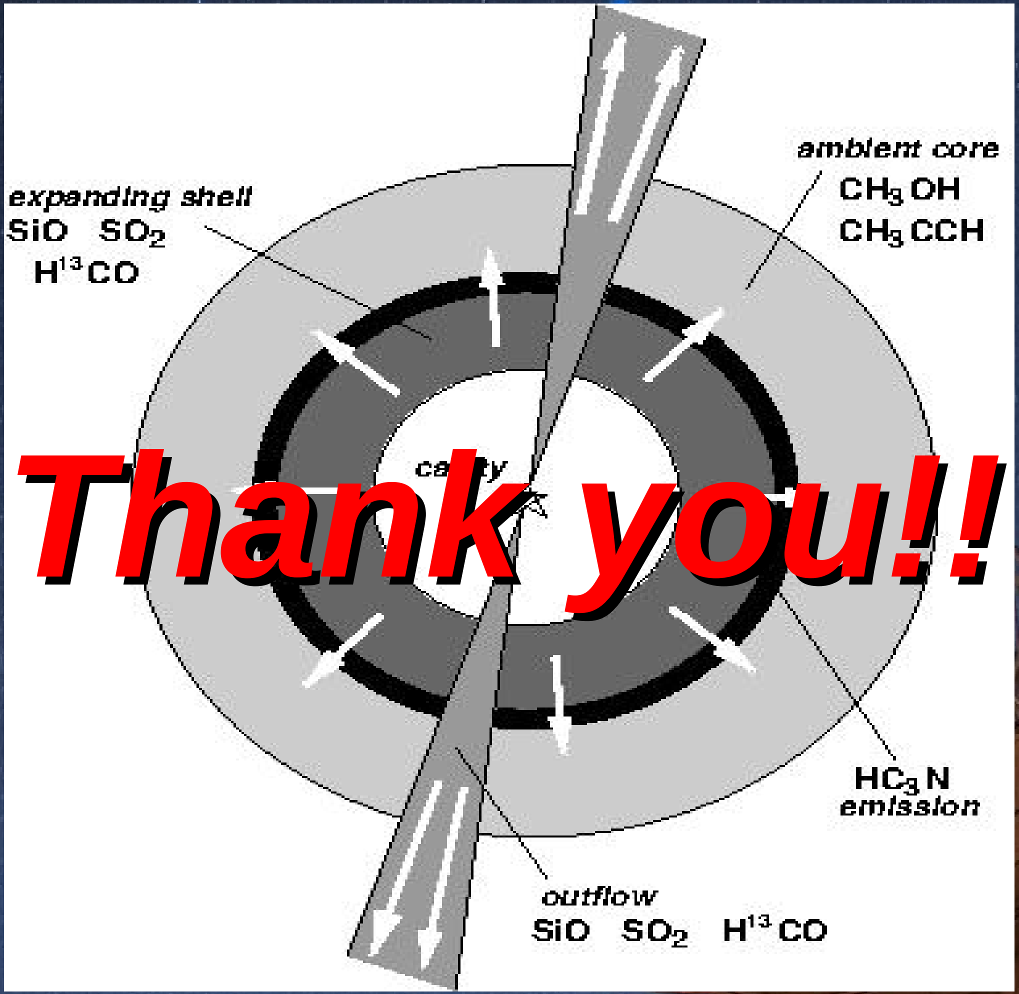

Thank you!!

ALLAM 2019. Astrochemistry LLAMA Meeting. Sao Paulo, August 8-9 2019. IAG-USP